

Article

Long-Term Spatiotemporal Characteristics of *Ulva prolifera* Green Tide and Effects of Environmental Drivers on Its Monitoring by Satellites: A Case Study in the Yellow Sea, China, from 2008 to 2023

Yating Zhan ^{1,2,3}, Zhongfeng Qiu ^{1,*} , Yujun Wang ^{2,3}, Yiming Su ^{2,3}, Yin Li ^{2,3}, Yanmei Cui ^{2,3}, Shuai Qu ^{2,3}, Peng Wang ^{2,3} and Xin Rong ^{2,3}

¹ School of Marine Sciences, Nanjing University of Information Science & Technology, Nanjing 210044, China; zhanyt0228@163.com

² Geological Survey of Jiangsu Province, Nanjing 210018, China

³ Natural Resources Satellite Application Technology Center of Jiangsu Province, Nanjing 210018, China

* Correspondence: zhongfeng.qiu@nuist.edu.cn

Abstract: *Ulva prolifera* (*U. prolifera*) green tide outbreaks have occurred in the Yellow Sea of China for many years, causing serious losses to marine ecology and the marine economy. The monitoring and tracking of *U. prolifera* green tide is a crucial aspect of marine ecological disaster prevention and control management. This paper aims to investigate the spatiotemporal distribution changes in *U. prolifera* green tide in the Yellow Sea throughout its life cycle. A survey of the Yellow Sea from 2008 to 2023 was conducted using multi-source remote sensing images. Long-term monitoring and analysis of *U. prolifera* revealed the evolution process of the green tide, including the early development, outbreak, decline, and extinction stages, considering time, space, and frequency of occurrence. Additionally, this study examined peak coverage change patterns over the past 16 years and analyzed the influence of environmental factors such as sea surface temperature and sea surface wind field on the development of *U. prolifera*. The research results serve as a valuable reference for the monitoring, early warning, and scientific prevention and control of *U. prolifera* green tide in the Yellow Sea, as well as other similar marine disaster areas.

Keywords: green tide; spatial and temporal evolution; interannual variation; Yellow Sea



Citation: Zhan, Y.; Qiu, Z.; Wang, Y.; Su, Y.; Li, Y.; Cui, Y.; Qu, S.; Wang, P.; Rong, X. Long-Term Spatiotemporal Characteristics of *Ulva prolifera* Green Tide and Effects of Environmental Drivers on Its Monitoring by Satellites: A Case Study in the Yellow Sea, China, from 2008 to 2023. *J. Mar. Sci. Eng.* **2024**, *12*, 630. <https://doi.org/10.3390/jmse12040630>

Academic Editor: Sang Heon Lee

Received: 28 February 2024

Revised: 1 April 2024

Accepted: 5 April 2024

Published: 8 April 2024



Copyright: © 2024 by the authors. Licensee MDPI, Basel, Switzerland. This article is an open access article distributed under the terms and conditions of the Creative Commons Attribution (CC BY) license (<https://creativecommons.org/licenses/by/4.0/>).

1. Introduction

Since 2008, *U. prolifera* has experienced seasonal outbreaks in the Yellow Sea of China for 16 consecutive years. This phenomenon involves extensive reproduction and aggregation in the waters of Jiangsu and Shandong provinces, resulting in the formation of a green tide. The green tide not only disrupts the marine ecosystem but also adversely affects coastal cities' aquaculture, aquafarming, tourism, and maritime transportation industries [1]. Consequently, these developments have inflicted significant economic losses on the region. Hence, the green tide has emerged as a significant marine ecological disaster in the Yellow Sea, garnering substantial public attention [2].

In response to the ecological disaster related to *U. prolifera* green tide in the Yellow Sea, experts and scholars from various fields, both domestically and internationally, have conducted extensive research from multiple perspectives [3]. This comprehensive inquiry encompasses the origin, developmental process, and interannual variations in *U. prolifera*, as well as its biological characteristics, outbreak mechanisms, ecological and environmental impacts, disaster prevention and mitigation, and resource utilization. Research efforts have included utilizing a combination of morphological and molecular biology techniques for sampling and comparative analysis of green algae in the Yellow Sea to study the origin of *U. prolifera* [2–4]. Furthermore, comprehensive remote sensing monitoring research has

been conducted to investigate the spatial development processes and interannual variations following the outbreak of *U. prolifera* [5–12]. Additionally, research has delved into the life history and reproductive characteristics of *U. prolifera* and elucidated the reasons for its dominance as the prominent green tide algae species [13–15]. Environmental factors such as sea temperature, salinity, sea surface flow fields, and the eutrophication of seawater, caused by the large amounts of nutrients carried by inland polluted water sources into the sea in the process of rapid industrial development in coastal cities, have also been explored to determine their influence on the outbreak of *U. prolifera* [16,17]. The impact of the *U. prolifera* outbreak on marine life and the ecological environment has likewise been scrutinized [18,19]. Additionally, research into disaster prevention and mitigation, including salvage and disposal [20,21], as well as resource utilization, in other parts of the world [22] has yielded a series of crucial scientific findings. Collectively, these research endeavors have laid the groundwork for the scientific prevention and control of *U. prolifera* in the Yellow Sea.

Studying the spatiotemporal distribution characteristics and evolutionary patterns of *U. prolifera* green tide is of paramount importance for early prevention and control. The temporal and spatial distribution, as well as the development of *U. prolifera*, are affected by various environmental factors and exhibit distinct interannual variations. While some domestic scholars have conducted remote sensing monitoring studies of the distribution characteristics of *U. prolifera* in individual years [9,11] and across multiple years [5,12], long-term remote sensing monitoring studies are scarce regarding the spatiotemporal distribution of *U. prolifera* over the years. Monitoring the spatiotemporal distribution of *U. prolifera* green tide over a longer time scale is necessary to analyze its outbreak mechanism and formulate prevention and control strategies accordingly. This paper systematically aggregates the outcomes of extensive operational remote sensing monitoring carried out by the Natural Resources Satellite Application Technology Center of Jiangsu Province over several years and retrospectively analyzes the *U. prolifera* outbreak processes in previous years. Based on the monitoring results, we undertake a comprehensive study of the spatiotemporal distribution and evolving characteristics of *U. prolifera* in the Yellow Sea over the years, aiming to provide a scientific foundation for the prevention, control, and management of *U. prolifera* in the Yellow Sea.

2. Materials and Methods

2.1. Study Area

The study area primarily covers the Yellow Sea, being specifically located within the coordinates of 32°~38° N and 119°~123° E, as shown in the yellow dotted box in Figure 1. This area encompasses the territorial seas of Jiangsu and Shandong provinces, as well as their offshore waters.

2.2. Data Source

This study conducted daily full-process monitoring of the historical outbreak of *U. prolifera* green tide in the Yellow Sea. It required regularly revisiting satellite images during the outbreak period, a large monitoring range, and high satellite space coverage capabilities. Therefore, it mainly used the HY-1C/D, TERRA, and AQUA satellite images, which have rapid revisiting, wide swath, and medium resolution. In addition, for the development stage of *U. prolifera* with small spatial patches, we supplemented a small number of domestically produced high-resolution images such as the GF1/6 and HJ-2A/B. For cloudy weather, we supplemented a small number of SAR images such as GF3 and RADARSAT-2 when optical images could not be effectively monitored. The main parameters and usage of the data sources are shown in Table 1.

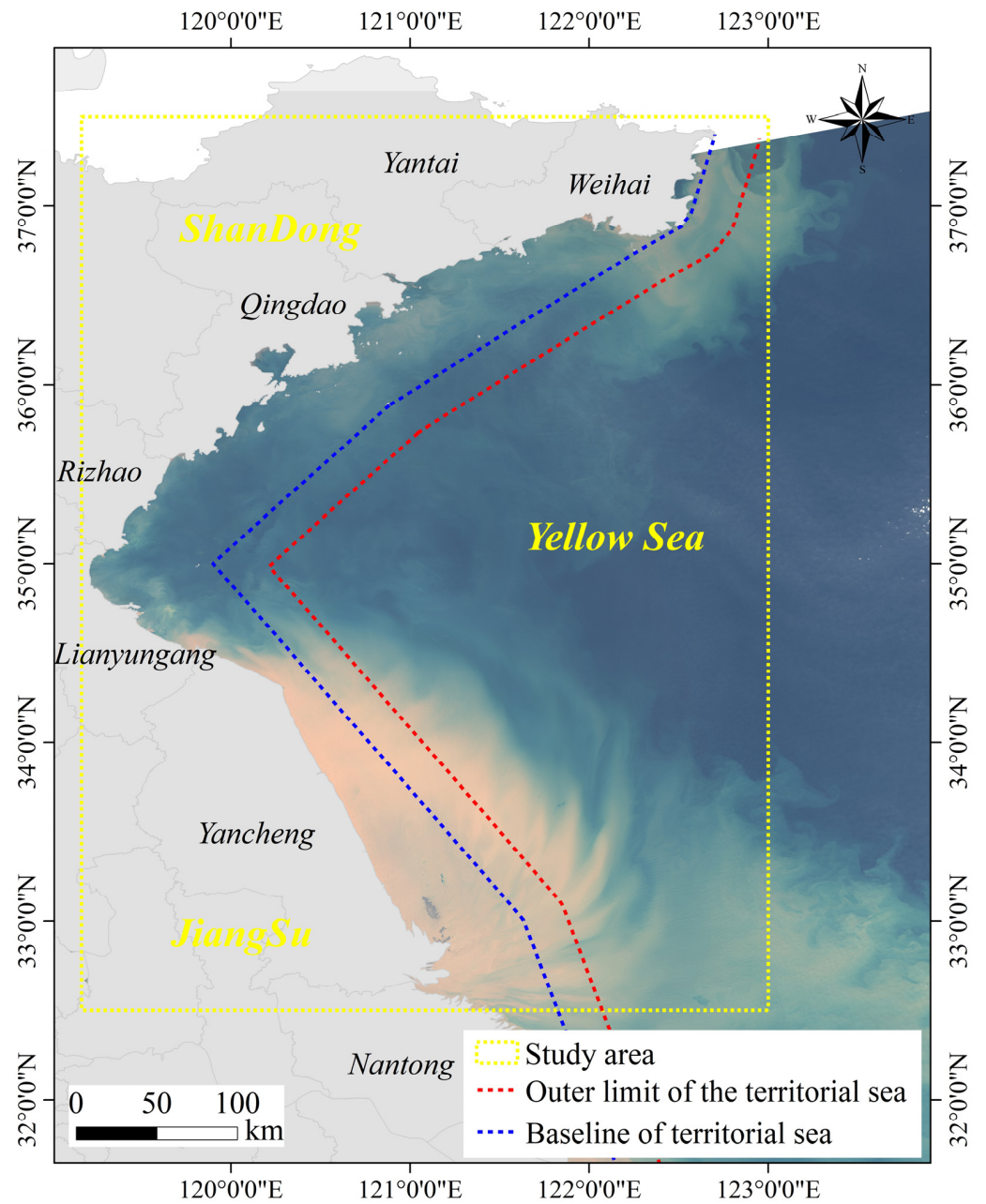


Figure 1. Study area of *U. prolifera* in the Yellow Sea.

Table 1. Related data source parameters of satellite remote sensing monitoring.

Satellite	Sensor	Resolution (m)	Frequencies Used
HY-1C, HY-1D	CZI	50	2019~2023
Terra, Aqua	MODIS	250	2008~2018
GF1, GF6	MUX	16	85 scenes
HJ-2A, HJ-2B	MUX	16	59 scenes
GF3, RADARSAT-2	SAR	10, 25	47 scenes

HY-1C/D are the first operational ocean water color satellites of China for earth observation [23], which mainly observe Chinese offshore and coastal areas. They were launched on 7 September 2018 and 11 June 2020, respectively. HY-1C’s descending equator crossing time is CST 10:30 am ± 30 min, and HY-1D’s ascending local time is 1:30 pm ± 30 min. It is equipped with a 4-band Coastal Zone Imager (CZI), providing blue (420~500 nm),

green (520~600 nm), red (610~690 nm) and near-infrared (760~890 nm) images. The double-satellite observation in the morning and afternoon can achieve high-frequency coverage 2 times every 3 days, with a 50 m spatial resolution and 950 km swath width. HY-1C/D has gradually replaced foreign remote sensing data sources with the advantages of high coverage frequency and relatively high spatial resolution. It has become the main data source for the operational remote sensing monitoring of *U. prolifera* green tide in the Yellow Sea in China [24,25]. Using the “China Ocean Satellite Data Service System” (<https://osdds.nsoas.org.cn/home>, accessed on 1 February 2024), the CZI online distribution time cost of the L1C-level product is less than 2 h, and it can realize near-real-time monitoring of *U. prolifera* green tide.

The TERRA satellite was launched in 1999, and the AQUA satellite was launched in 2002. Both satellites are equipped with a Moderate-Resolution Imaging Spectroradiometer (MODIS). The single-star revisit period is 1 day. TERRA is a morning star, and AQUA is an afternoon star. From the official website of NASA (<https://ladsweb.modaps.eosdis.nasa.gov/>, accessed on 1 February 2024), we obtained 500 m blue (459~479 nm) and green (545~565 nm) images, as well as 250 m red (620~670 nm) and near-infrared (841~876 nm) images. Then, the blue and green bands were resampled to 250 m.

2.3. Method

U. prolifera has similar spectral characteristics to vegetation. It appears green on true color images (a combination of red, green, and blue bands) and appears red on standard false-color images (a combination of near-infrared, red, and green bands), as shown in Figure 2a,b, respectively. Domestic and foreign scholars have proposed many algorithms for the remote sensing monitoring of *U. prolifera*, most of which use the spectral index method. The more commonly used ones include the normalized difference vegetation index (NDVI) [26], enhanced vegetation index (EVI), floating algae index (FAI) [27], alternative floating algae index (AFAI) [28], etc. The monitoring capabilities of the four commonly used spectral indices for *U. prolifera* were analyzed [29], and the results showed that the NDVI algorithm had the strongest monitoring ability for each stage of the *U. prolifera* disaster. The NDVI further amplified the difference in reflectivity of *U. prolifera* in the near-infrared and red bands (Figure 2c) and identified *U. prolifera* stably and reliably. This paper also used the NDVI index to extract *U. prolifera*, and its expression was as follows:

$$NDVI = \frac{NIR - R}{NIR + R}$$

where *NIR* and *R* are the reflectance of near-infrared and red bands, respectively.

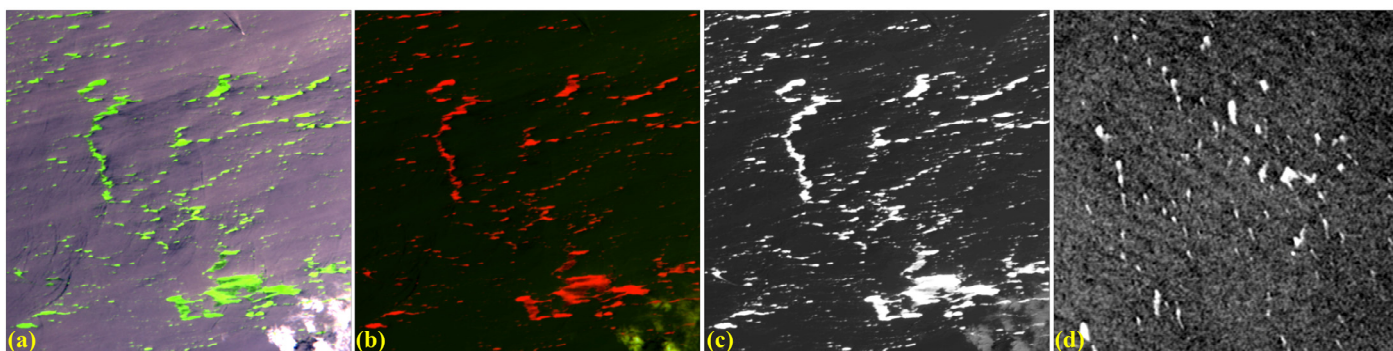


Figure 2. Characteristics of *U. prolifera* and seawater on different images: (a) true-color image; (b) standard false-color image; (c) NDVI image; (d) SAR image.

The theoretical threshold for extracting *U. prolifera* using the NDVI index is 0, but it is affected by differences in sensors, band channels, marine environments such as wind and waves, and cloud coverage, resulting in small-scale fluctuations in the extraction threshold.

Therefore, this paper uses the maximum inter-class variance [30] based on local image differences. The algorithm calculates the optimal threshold for a specific optical satellite image, which is the NDVI segmentation threshold shown in Figure 3a, to perform adaptive *U. prolifera* extraction.

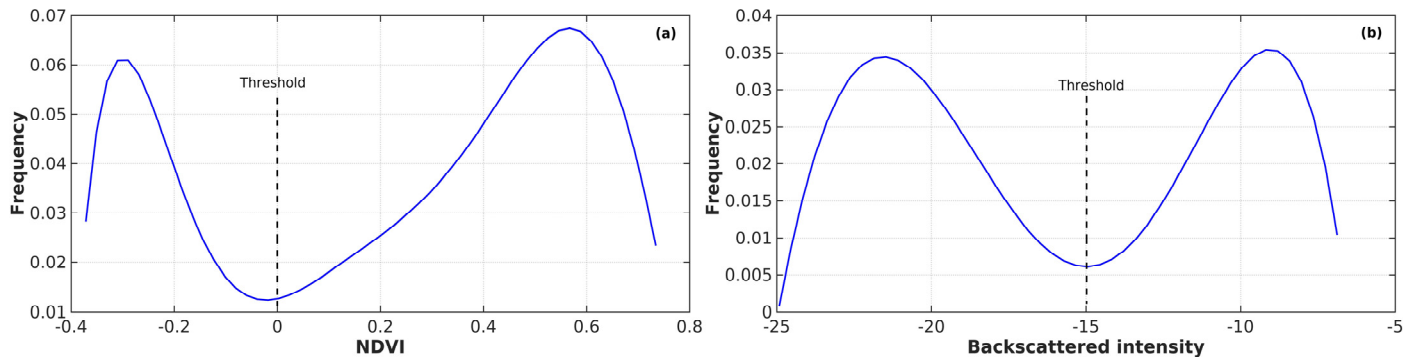


Figure 3. Distribution histogram curve (blue solid line) of *U. prolifera* and seawater in satellite remote sensing images: (a) histogram of NDVI; (b) histogram of backscattered intensity in SAR image.

In SAR images, due to the difference in backscattering between *U. prolifera* and seawater, there is an obvious brightness difference (Figure 2d). Compared with seawater, *U. prolifera* has a higher backscattering intensity and has a brighter appearance on the image [31]. For high brightness, the maximum inter-class variance algorithm is also used to calculate the optimal threshold (Figure 3b) for adaptive *U. prolifera* extraction for a specific SAR image; the backscattered intensity segmentation threshold is shown in the Figure 3b.

2.4. Area Calculation

U. prolifera at different stages of evolution shows different floating aggregation states on the sea surface. The sum of the areas of *U. prolifera* pixels extracted using the above method was used as the coverage area of *U. prolifera* to represent the true coverage of *U. prolifera* on the sea surface. However, due to the fragmentation of the *U. prolifera* distribution characteristics, the actual affected sea area was greater than the algae coverage area. Based on the extracted *U. prolifera* cover vector, this paper used the aggregation analysis tool in ArcMap to calculate the outer envelope surface of the coverage vector, thereby calculating the *U. prolifera* distribution area to characterize *U. prolifera*.

When using different images to monitor the *U. prolifera* coverage area, there were often significant differences in the extracted coverage areas due to the comprehensive influence of the image's spatial resolution, band settings, sensor differences, and other factors. Among them, spatial resolution is the main factor affecting the area difference. The comparison of the coverage areas of different spatial resolutions revealed that the lower the spatial resolution, the larger the extraction coverage [32]. The extraction area of relatively high-resolution images was closer to the true value [33]. This paper used 50 m CZI and 250 m MODIS data as the main image sources over the entire period of *U. prolifera* monitoring. To ensure the consistency of the area extraction results between CZI and MODIS, the results of the two sensors needed to be unified. The most common method is to select a reference date for a cloud-free and better sea surface environment. Based on the reference date, the coverage areas were extracted, respectively, and then the unified coefficient was retrieved as the area ratio between CZI and MODIS. Subsequently, the unified coefficient was multiplied by every MODIS area to obtain the same benchmark as the CZI extraction area [33]. This paper used this method to ensure the continuity of monitoring results from different sources.

3. Results and Discussion

Based on the images of cloudless or cloud-free dates during 16 entire life cycles of *U. prolifera* and the above methods, a series of key information was identified, as shown in

Table 2. The results include the initial date observed via remote sensing, the main body of *U. prolifera* crossed over the border between Jiangsu and Shandong seas, annual peak areas, the final extinction date, and green tide lasting days. In addition, the key date distribution of *U. prolifera* development over the 16 years studied is shown in Figure 4.

Table 2. Remote sensing monitoring results of the green tide in the Yellow Sea from 2008 to 2023.

Years	First Appearance Date	Peak Coverage Date	Peak Coverage Area (km ²)	Peak Distribution Area (km ²)	Demise Date	Duration Days
2008	10 May	28 Jun	633	17,828	19 Aug	102
2009	27 May	15 Jul	848	23,419	31 Aug	97
2010	2 Jun	6 Jul	485	29,199	9 Aug	69
2011	1 Jun	19 Jun	555	12,472	22 Aug	83
2012	17 May	6 Jul	120	10,125	23 Aug	99
2013	22 May	29 Jun	674	16,638	19 Aug	90
2014	15 May	28 Jun	875	29,472	22 Aug	100
2015	20 May	21 Jun	581	56,310	14 Aug	87
2016	19 May	17 Jun	562	51,862	4 Aug	78
2017	18 May	17 Jun	299	36,126	26 Jul	70
2018	23 May	21 Jul	179	25,062	24 Aug	94
2019	12 May	5 Jul	447	58,019	9 Sep	121
2020	27 May	14 Jun	176	15,216	1 Aug	67
2021	21 May	19 Jun	1598	59,440	25 Aug	97
2022	16 May	24 Jun	240	24,787	26 Aug	103
2023	9 May	22 Jun	939	53,644	26 Aug	110

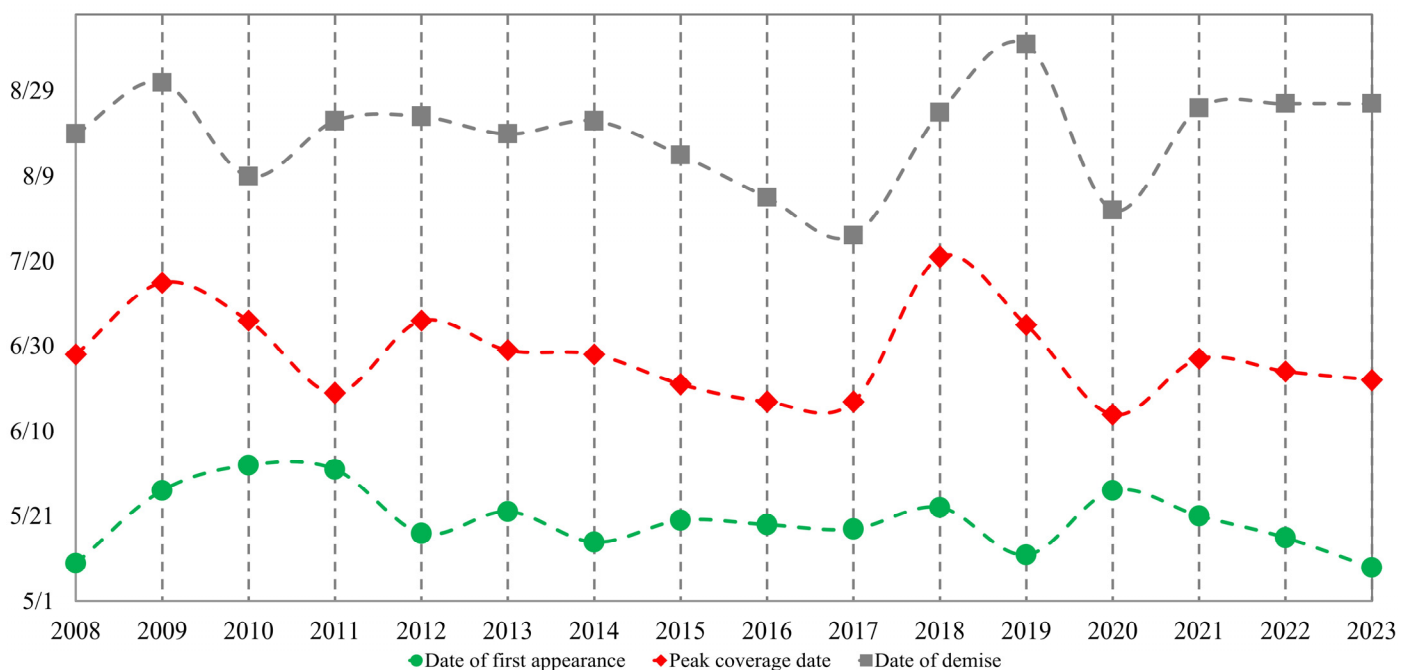


Figure 4. Series of green tide evolutionary key dates of *U. prolifera* in the Yellow Sea from 2008 to 2023.

It is worth mentioning that the earliest occurrence of *U. prolifera* was detected in 2007. However, due to the lack of cloud-free or cloudless images, as well as the very small scale of the outbreak, accurate information for 2007 cannot be completely obtained. Therefore, Table 2 shows the development information for *U. prolifera* from 2008.

3.1. Temporal Distribution Characteristics

From the perspective of the first appearance date, peak coverage area, and demise date of *U. prolifera*, as shown in Table 2, obvious differences exist in the scale of the outbreaks in different years. The principles causing these differences are complex, and some studies have pointed out that it is mainly related to environmental factors such as sea temperature [16], nutrients, marine climate [17], etc. Among them, the duration of 121 days in 2019 was the longest in the past, and 67 days in 2020 was the shortest. The average duration was about 92 days. Although the duration and coverage of *U. prolifera* outbreaks varied in different years, the overall evolution process generally went through relatively similar stages, as it usually appeared in the summer and entered a rapid outbreak period after a period of development, reached peak coverage and maintained it for a short period of time, then began to enter the period of extinction. Affected by the severe cloud cover in summer, most of the daily results could only be monitored partially, and the full coverage area could be monitored every ten days on average, so the average maximum coverage area in each ten-day session from May to August was calculated and is shown in Figure 5. Based on the change characteristics of the coverage area during this period, we divide the overall evolutionary process into the following four stages:

- (1) Development stage: The monitoring results from the past 16 years show that satellite remote sensing detected the first emergence of *U. prolifera* in early and mid-May. Combined with the on-site drone survey results, the early *U. prolifera* coverage area was small and often appeared in the form of a mixed growth of Sargassum (in Figure 6a, brown is Sargassum and green is *U. prolifera*). Compared with other algae, *U. prolifera* has a strong ability to absorb nutrients and can utilize inorganic and organic nitrogen and phosphorus to achieve rapid growth [17,34]. The higher nutrient content in the coastal waters of the Yellow Sea provides rich nutrients for the growth of *U. prolifera* [35,36], coupled with the impact of rising sea surface temperatures, so the growth and reproduction of *U. prolifera* accelerates and gradually appears in sporadic flowers and spatially discrete distribution (Figure 6b). The average maximum coverage area in mid-May is about 33 km².
- (2) Outbreak stage: Upon gradually entering the outbreak period, the coverage area doubled, and *U. prolifera* was spatially clustered into large patches (Figure 6c). It reached the annual peak coverage from late June to early July and was further spatially aggregated into a strip shape (Figure 6d), forming a large-scale green tide that stretched from several kilometers to tens of kilometers and gradually reached the nearshore beach (Figure 6e). In late May, the annual average maximum coverage area was about 109 km², and by late June, this number was about 517 km².
- (3) Decline stage: The coverage area gradually entered the decline period in July. As the sea temperature further rose and exceeded the suitable growth temperature of *U. prolifera*, reproduction begins to slow down. In addition, *U. prolifera* gradually approached the coast affected by the wind field on the sea surface and was salvaged, organized by the local management department, and the coverage area decreased rapidly by late July. It can be seen that the reduction rate was relatively consistent with the growth rate of the outbreak stage. By late July, the average maximum coverage area over the years was about 109 km².
- (4) Extinction stage: In August, the coverage area continued to decrease and entered the extinction period, and the complete extinction date was mostly concentrated in the mid-to-late August.

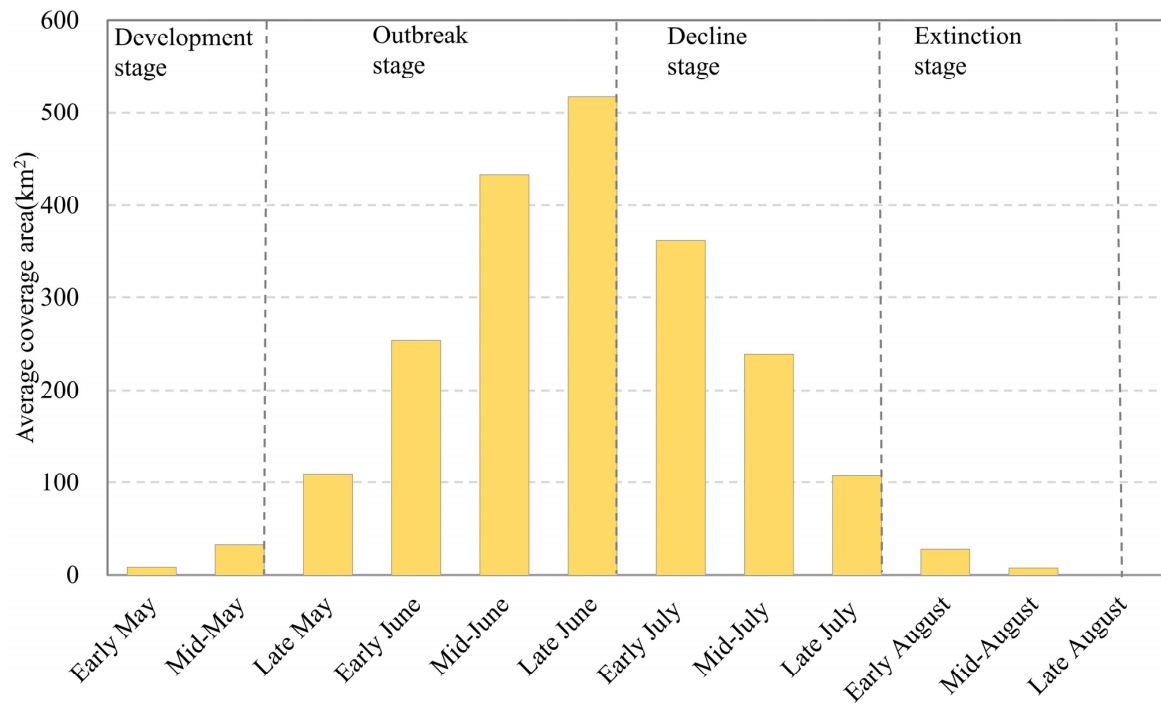


Figure 5. The average distribution of the maximum coverage of *U. prolifera* from May to August in 2008–2023.

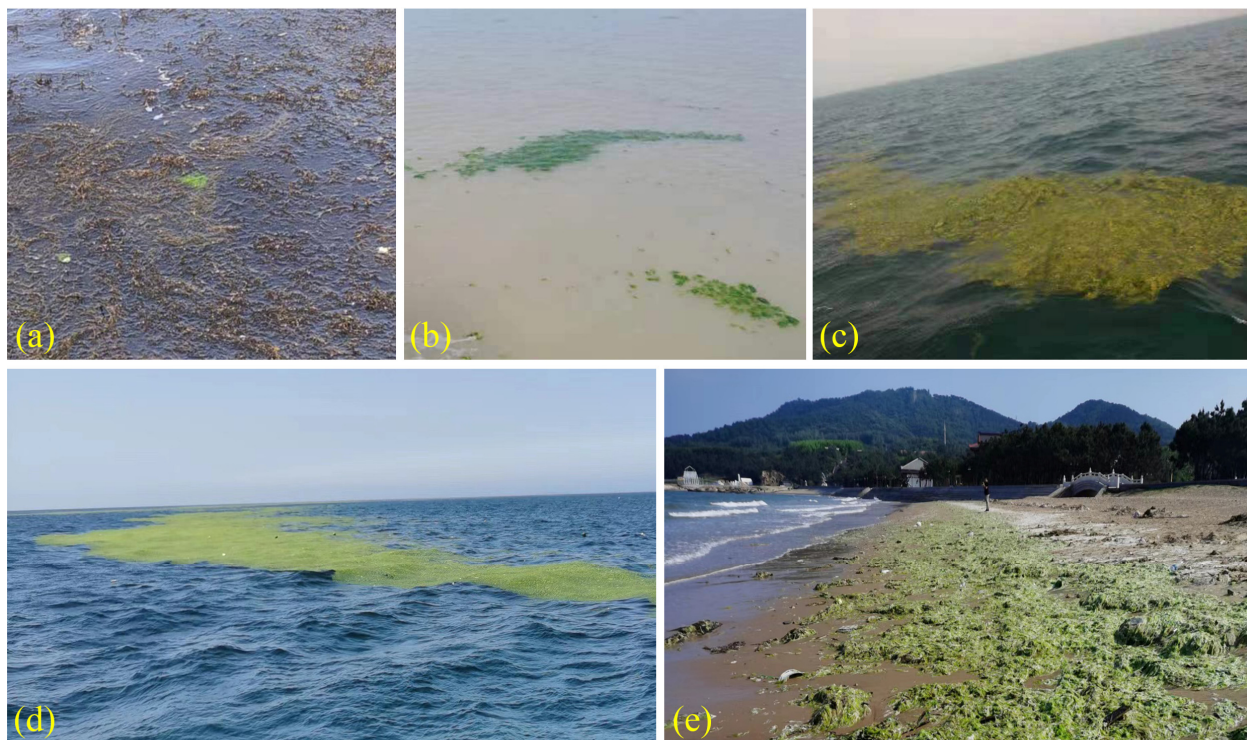


Figure 6. Spatial patterns of different evolutionary stages of *U. prolifera*: (a) *U. prolifera* (green) mixing with Sargassum (brown); (b) sporadic and discrete shape; (c) large patchiness; (d) aggregation of strip; (e) nearshore beaching.

3.2. Spatial Distribution Characteristics

The green tide of *U. prolifera* in the Yellow Sea mainly occurs in summer. Under the influence of sea surface monsoons and flow fields, floating *U. prolifera* undergoes spatial

movement through complex ocean processes [1], resulting in early development, outbreak, decline, and extinction. In different sea areas, the spatial migration distance is hundreds of kilometers.

Due to differences in the spatiotemporal distribution of sea surface wind fields and flow fields, the movement of *U. prolifera* in a short period is more complicated [25]. However, there is a high similarity in the direction of spatial development in relatively longer time scales such as ten days and months. The geometric center of the distribution of *U. prolifera*, connected in chronological order, represents the development direction of the spatial distribution of *U. prolifera* and can be used to analyze the spatial development rules of *U. prolifera* over the years. The spatial development directions of *U. prolifera* from 2008 to 2023 are shown in Figure 7; according to the changes in development direction, we divided them into the following two types:

- (1) Northward development type: In the early development stage, it was mostly found in the eastern sea of Yancheng in northern Jiangsu. The distribution center gradually moved from the eastern sea of Yancheng either to the north directly or first to the northwest and then to the northeast along the coastline. Finally, it reached the urban sea area along the southern Shandong Peninsula. During the peak period, the main body of *U. prolifera* was distributed in the Shandong Sea, which is mainly located on the coast around the Lianyungang, Rizhao, and Qingdao seas. The development directions in 2008, 2010, 2013, 2015, 2017, 2018, and 2023 belong to this type.
- (2) Northward in the early stage and southward in the later stage development type: When entering the decline and extinction periods, the distribution center of *U. prolifera* gradually moved southward, from the Qingdao Sea area to the Rizhao Sea area, and went a step further to the junction area around the Jiangsu–Shandong border. The process of southward movement in different years was relatively similar. It should be noted that the movement of the distribution center in the extinction period was different from those in the other periods. Variations in the distribution center in the extinction period over the years were mainly related to the extinction time sequence and decreasing rate in each sea area. The overall result over the years shows that the distribution center of *U. prolifera* during the outbreak period was mostly located in the sea area of Qingdao, while the final extinction area was mostly located in Rizhao, as well as in the Jiangsu–Shandong border area. The development directions in other years belong to this type.

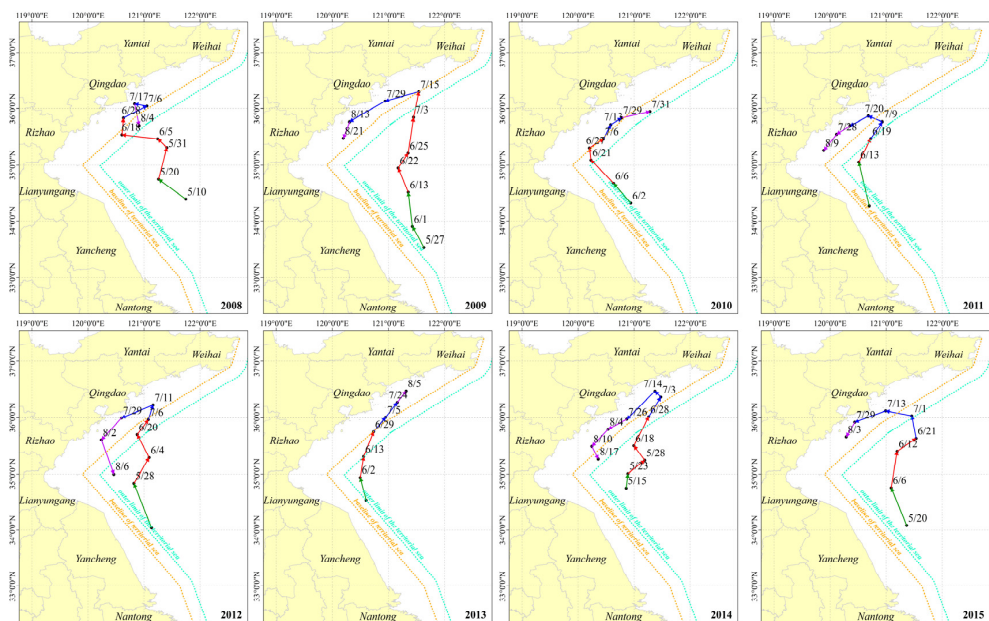


Figure 7. Cont.

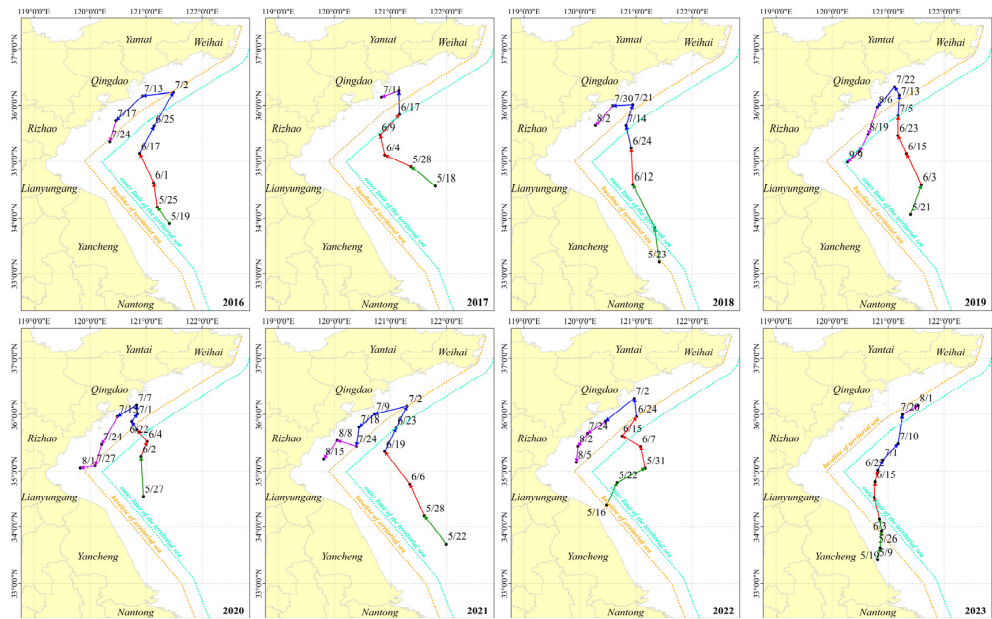


Figure 7. Spatial migration direction of *U. prolifera* in the Yellow Sea from 2008 to 2023. Green solid arrow indicates development stage, red solid arrow indicates outbreak stage, blue solid arrow indicates decline stage, and purple solid arrow indicates extinction stage.

3.3. Frequency Characteristics

To compare the outbreak level of *U. prolifera* in different sea areas of the Yellow Sea, the interannual distribution frequency of the peak distribution ranges was calculated via a spatial overlay analysis tool using the geographic information system software ARCMAP (version 10.2) from 2008 to 2023. The higher the distribution frequency, the more serious the outbreak level of *U. prolifera*. Figure 8 shows the spatial distribution frequency of peak coverage between different years in the Yellow Sea.

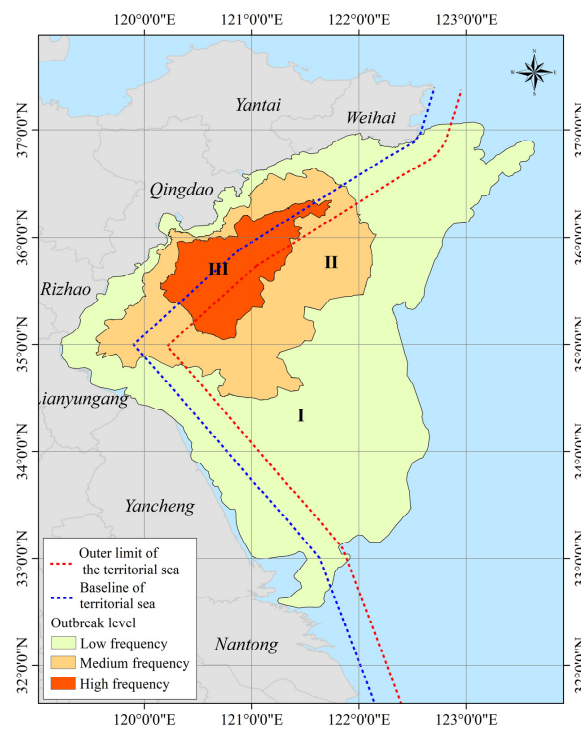


Figure 8. Spatial occurrence levels of *U. prolifera* in the Yellow Sea from 2008 to 2023. Area I: low-frequency; Area II: medium-frequency; Area III: high-frequency.

The overall outbreak sea areas over the years were mainly located between 33° and 37° N and west of 123° E, with the total affected sea area being 95,815 km². According to the distribution frequency, the affected areas were classified into three grades. Area III was a high-frequency distribution, that is, 11 to 16 times, mainly located around the terrestrial sea baseline (dot-blue line in Figure 8) from Rizhao to Qingdao. The distribution of area III was 9050 km², accounting for about 9.4%. Area II was a medium-frequency distribution, that is, 6~10 times, located in the seas on both sides of the terrestrial sea outer line (dot-red line in Figure 8) from Lianyungang to Yantai, with a sea area of 22,101 km², accounting for about 23.1% of the total quantity. Area I was a low-frequency distribution, that is, 1 to 5 times, located in the sea areas from Yancheng to Weihai, with a sea area of 64,664 km², accounting for about 67.5% of the total. The scope of the three divisions gradually shrank from the far sea to the offshore sea, and the level of impact gradually increased. It can be concluded that the coast from Qingdao to Yantai was the area most severely affected by *U. prolifera*.

3.4. Interannual Peak Comparison

Although the annual spatial and temporal development and evolution of *U. prolifera* green tide in the Yellow Sea are relatively similar, the biomass of floating *U. prolifera* is affected by a variety of marine environmental factors, such as sea temperature, nutrients, freshwater input, and competition with other species of algae [34–36]; there are large differences in the peak coverage area and distribution area of *U. prolifera* in each year (Figure 9).

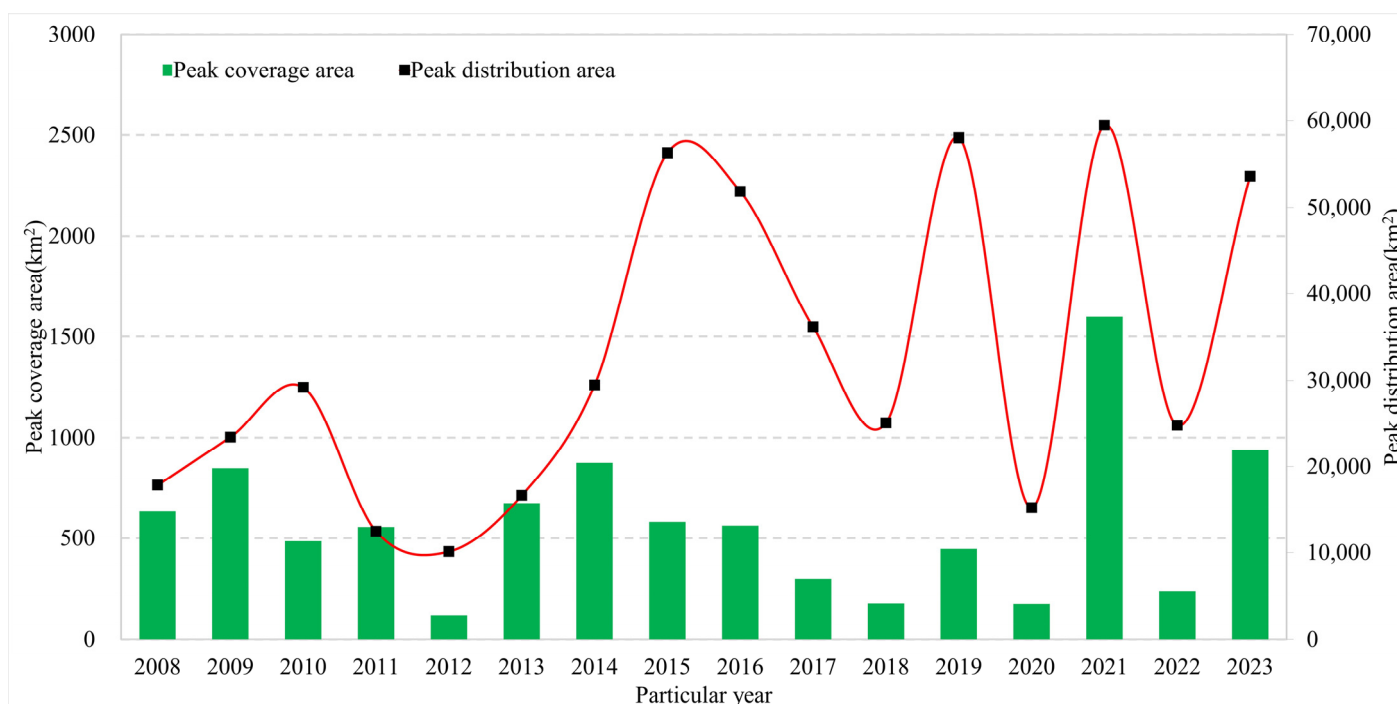


Figure 9. Changes in the peak coverage and distribution area of *U. prolifera* in the Yellow Sea from 2008 to 2023. The distribution area data connection is represented by a red line.

The average peak coverage area from 2008 to 2023 was 517 km², for which the historical minimum of peak coverage area was 120 km² in 2012, and the historical maximum of peak coverage area was 1598 km² in 2021. Comparatively, the average peak distribution area over the years was 32,476 km², for which the historical minimum of peak distribution area was 10,125 km² in 2012, and the historical maximum of peak distribution area was 59,440 km² in 2021.

Except for 2021, the peak coverage areas in the other years were less than 1000 km². At the end of April 2021, extreme weather, that is, strong winds and thunderstorms, occurred in the seaweed breeding area on the sandbank in northern Jiangsu, resulting in the collapse of the raft frame of the breeding enterprise. Consequently, a large amount of green algae attached to the frame flowed into the sea and caused the highest level outbreak ever of *U. prolifera*, far higher than in other years.

It was found from the peak coverage areas over the years that the scale of outbreaks in recent years has been at a high level. The historical maximum value was 1598 km² in 2021, and the secondary maximum was 939 km² in 2023; with two large-scale outbreaks occurring in such a short period of time, the mechanism behind this deserves further study.

3.5. Effects of Environmental Drivers

The occurrence, development, and evolution of *U. prolifera* are affected by various environmental factors, such as temperature, nutrients, ocean circulation, and climate change [20]. Among them, temperature is an important environmental factor that affects the development of *U. prolifera* and has a significant impact on the germination and growth rate of microscopic propagules [16,37]. The sea surface monsoon is the main driving force behind the long-distance spatial migration of *U. prolifera* and is also the main factor that affects its spatial migration and direction of development [38].

Ocean dynamic satellite data were used to invert the average sea surface temperature and sea surface wind field in each ten-day period from May to August. There are certain changes in the summer monsoon and sea surface temperature in the Yellow Sea. Taking 2023 as an example, as shown in Figure 10, the sea surface temperature began to rise slowly in early May and reached the maximum level in mid- and late August, with spatial trends decreasing from south to north. The temperature near the shore was slightly higher than that in the open sea. The sea surface wind field was mainly dominated by the northward monsoon along the coastal lines to the northwest and northeast. The spatial development direction of *U. prolifera* was highly consistent with the distribution and changes in the sea surface wind field. Relevant research data also confirm this view. The drift path of *U. prolifera* green tide has obvious interannual variation, and the change in the ocean surface flow field caused by the interannual variation in the sea surface wind field is considered to be the main reason for the variation in the *U. prolifera* transport path [17,39].

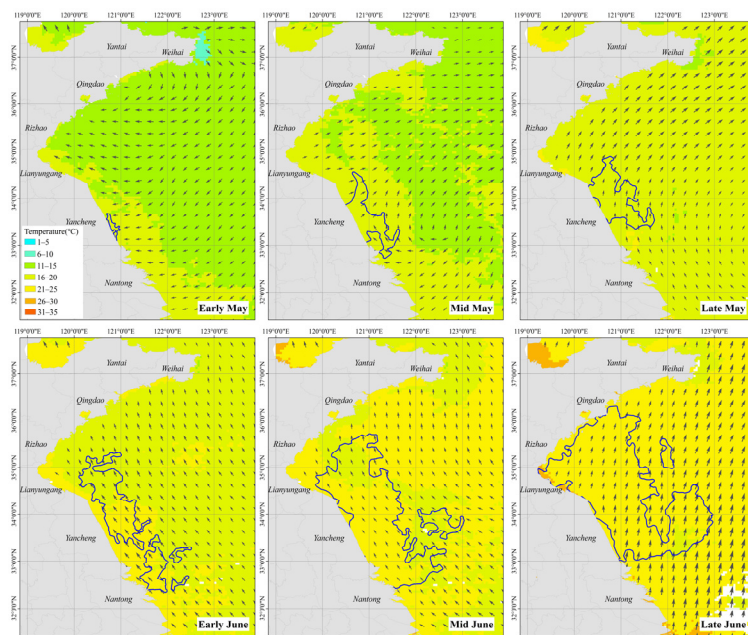


Figure 10. Cont.

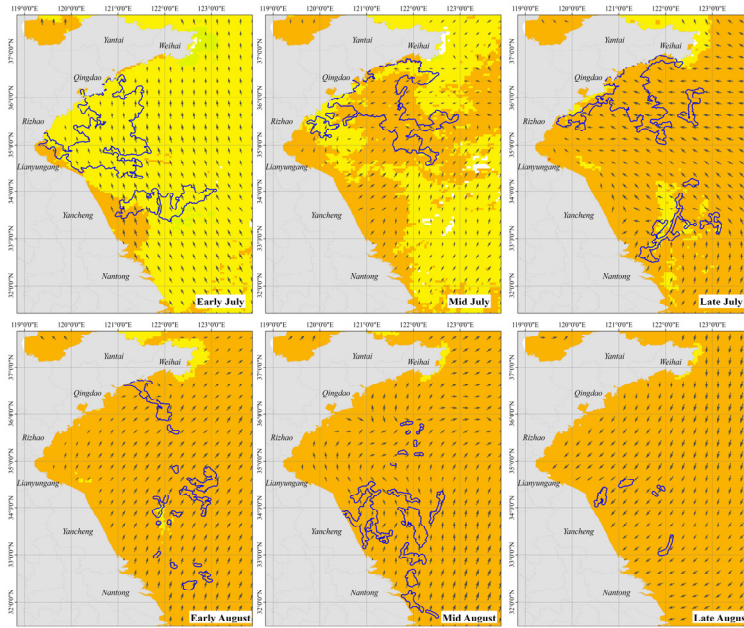


Figure 10. Sea surface temperature, sea surface wind field, and spatial distribution of *U. prolifera* in the Yellow Sea from May to August 2023. The 1st to 4th rows are for May to August, and the 1st to 3rd columns are early, middle, and late 10-day periods, respectively. The blue polygon represents the spatial distribution of *U. prolifera*, and the black arrow represents the sea surface wind field.

The correlation analysis between sea surface temperature and coverage area is helpful for understanding the effect of temperature on the development of *U. prolifera*. The sea surface temperature experiences fluctuations in a short period of time, and there is also a certain interannual variation, as shown in Figure 11; in order to obtain more robust statistical results, the correlation coefficient between the annual average sea temperature and *U. prolifera* coverage area was analyzed in units of ten days.

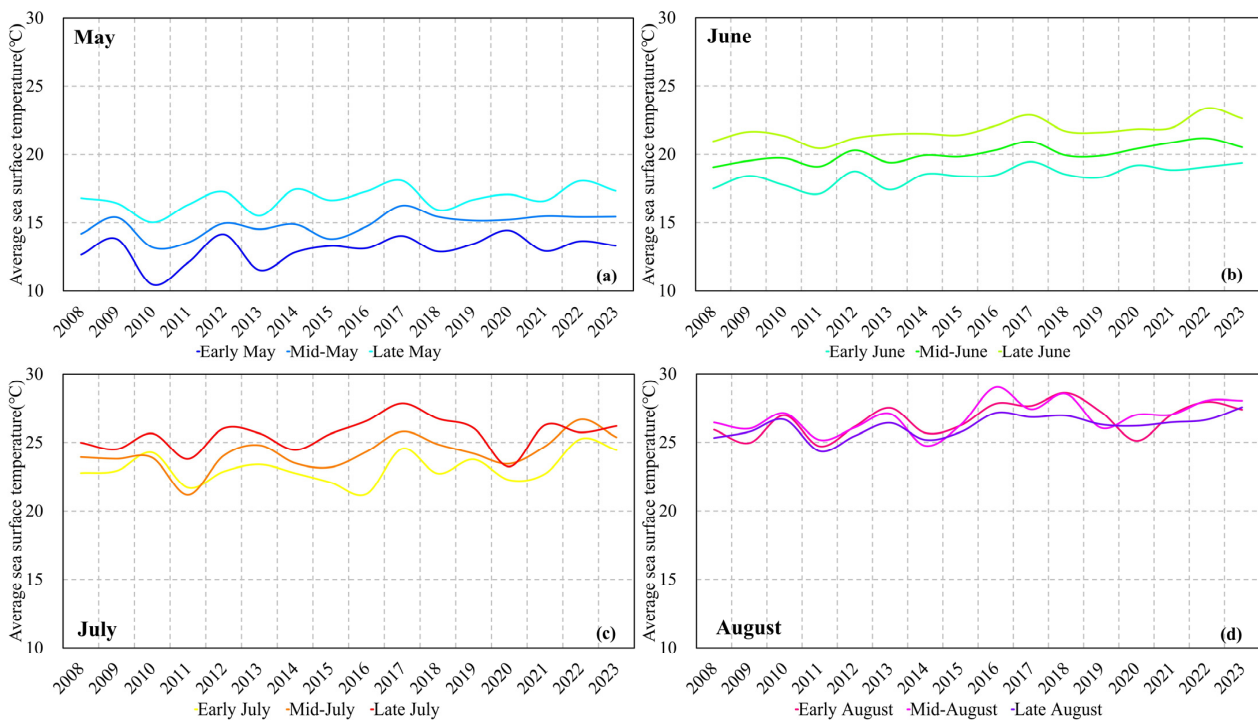


Figure 11. Sea surface temperature in the Yellow Sea from May to August in 2008–2023.

In the early and outbreak stages of *U. prolifera*, the sea surface temperature and the coverage area were both increasing, as shown in Figure 12b, and their correlation coefficient was 0.97. In the decline and extinction stage, the sea surface temperature continued to rise, while the coverage area began to shrink, resulting in a correlation coefficient of -0.98 , as shown in Figure 12c. Both of the two correlation coefficients indicated that temperature has an important influence on the growth of *U. prolifera*. Similar results were obtained in the study of the effect of temperature on the germination rate of *U. prolifera* micro propagules. The *U. prolifera* micro propagules could not germinate below $5\text{ }^{\circ}\text{C}$, and the germination rate was higher at $10\text{--}26\text{ }^{\circ}\text{C}$. The germination rate decreased significantly when the temperature continued to rise, and the germination almost stopped when the temperature exceeded $30\text{ }^{\circ}\text{C}$ [16,40]. Specifically, the development stage began in early and mid-May, in which period the average sea temperature over the years was between $14\text{ }^{\circ}\text{C}$ and $16\text{ }^{\circ}\text{C}$ and the growth rate was relatively slow. During the outbreak stage from late May to late June, the average sea temperature over the years was between $17\text{ }^{\circ}\text{C}$ and $22\text{ }^{\circ}\text{C}$. The growth rate in this period increased significantly. During the decline stage from early to late July, the historical average sea temperature was between 23 and $26\text{ }^{\circ}\text{C}$, but the coverage area decreased rapidly. During the extinction period in August, the historical average sea temperature began to rise higher than $26\text{ }^{\circ}\text{C}$. To sum up, the suitable temperature of *U. prolifera* growth was between $14\text{ }^{\circ}\text{C}$ and $26\text{ }^{\circ}\text{C}$, among which the growth rate achieved the fastest growth when the sea temperature ranged from $17\text{ }^{\circ}\text{C}$ to $22\text{ }^{\circ}\text{C}$.

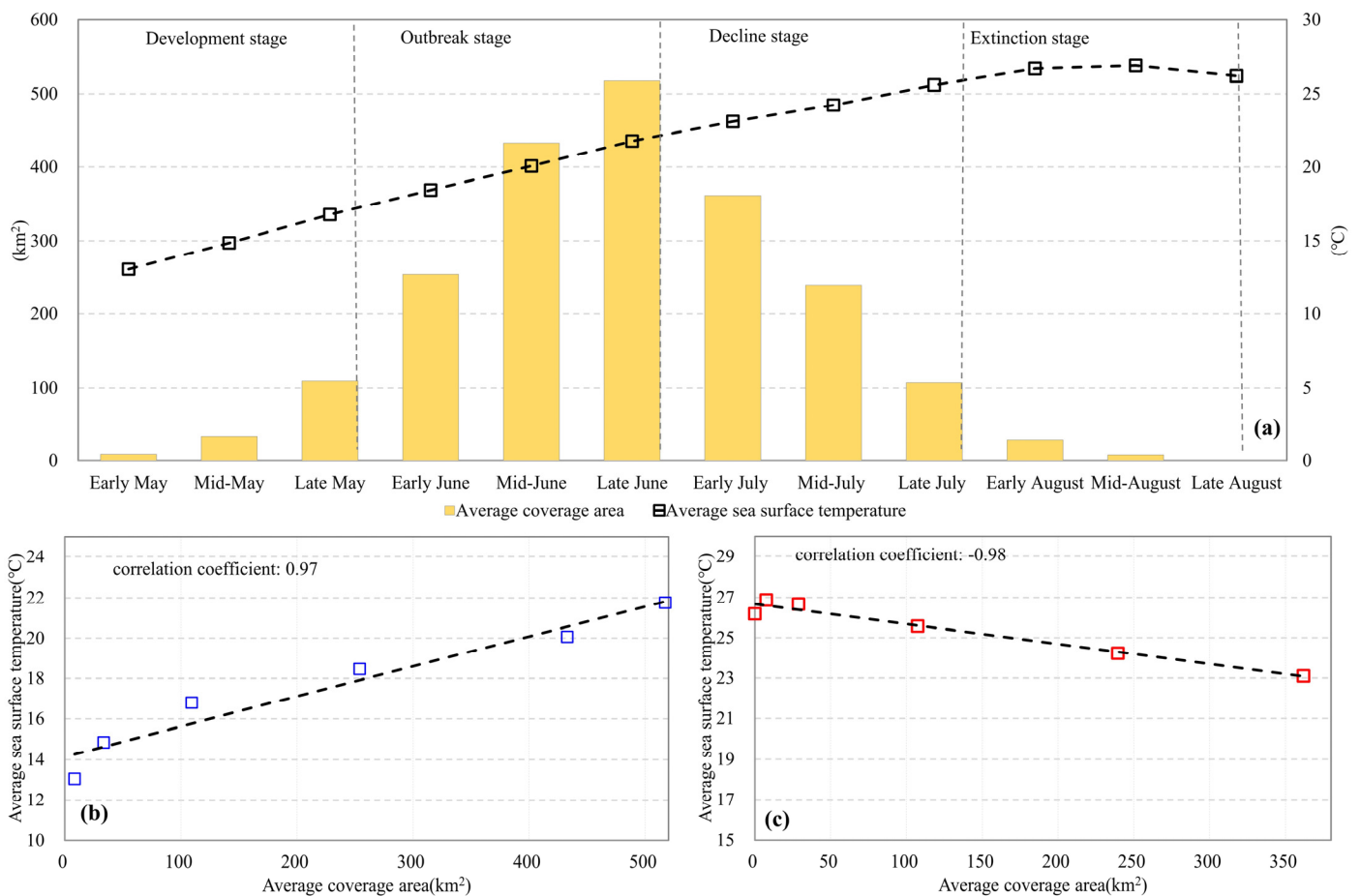


Figure 12. Distribution of average coverage area and average sea surface temperature: (a) average series of coverage area and sea temperature from May to August in 2008–2023; (b) correlation in the development and outbreak stage of average series in blue boxes; (c) correlation in the decline and extinction stage of average series in red boxes.

The outbreak of *U. prolifera* green tide is controlled by a variety of environmental factors. Nutrients in seawater are the life material basis, usually considered to be closely related to the formation of green tide [41,42]. Sea surface temperature is an important environmental factor affecting the germination rate of microscopic propagules [16,40]. Summer monsoon and surface ocean currents are the main driving forces behind the spatial drift [17,39]. These factors jointly affect the outbreak scale and spatial and temporal distribution of *U. prolifera*.

4. Conclusions

Comprehensive use of multi-source remote sensing images, sea surface temperature, sea surface wind field, and other data from 2008 to 2023 was conducted to study and analyze the spatiotemporal distribution characteristics, interannual changes, environmental driving effects, etc., of *U. prolifera* green tide in the Yellow Sea, and the following conclusions were drawn:

- (1) *U. prolifera* has mainly gone through four stages over the years: the development stage in early and mid-May, the outbreak stage from late May to late June, the decline stage in July, and the extinction stage in August. The average number of days that it has lasted over the years is 92 days, and the corresponding average peak coverage area is about 517 km².
- (2) The spatial distribution of *U. prolifera* over the years mainly includes a northward expansion stage and another southward contraction stage. It was first discovered in the waters of Yancheng, northern Jiangsu. Affected by the Yellow Sea monsoon, it develops and migrates overall either to the north directly or first to the northwest and then to the northeast. During the peak coverage period, it was mainly located in the offshore waters from Lianyungang to Qingdao. The peak coverage distribution over the years shows that the sea area affected by *U. prolifera* reaches as much as 9050 km², mainly located in Qingdao waters.
- (3) Occurrence frequency analysis shows that a low-frequency distribution makes up about 67.5%, medium-frequency distribution accounts for about 23.1%, and high-frequency distribution makes up about 9.4%. The scope of the three divisions gradually shrinks from the far sea to the offshore sea, and the level of impact gradually increases.
- (4) Comparison of interannual peak coverage areas shows that since 2018, the peaks and troughs of peak coverage areas have shown signs of alternate change year by year, and the peak coverage areas in 2021 and 2023 were both at historical highs.
- (5) Analysis of the average sea temperature and *U. prolifera* coverage area in each ten-day from May to August shows that the spatial development direction of *U. prolifera* is highly consistent with the distribution and changes in the sea surface wind field. The suitable growth temperature of *U. prolifera* is between 14 °C and 26 °C, among which the growth rate of *U. prolifera* was fastest when temperatures ranged from 17 °C to 22 °C.

Based on our findings, the spatial and temporal distribution, interannual variation, and the influence of sea temperature and wind field on the long-term green tide of *U. prolifera* in the Yellow Sea are revealed, which have important reference value for the scientific prevention and control of green tide. It remains a challenge to uncover the role of nutrients in the outbreak of *U. prolifera*. A comprehensive investigation into the nutrients would be appropriate for a future study to fully understand the driving mechanism of environmental factors.

Author Contributions: Conceptualization, Z.Q.; Data curation, S.Q., P.W. and X.R.; Formal analysis, Y.Z. and Z.Q.; Investigation, Y.Z.; Methodology, Y.L. and Y.C.; Study design, Y.W. and Y.S.; Data analysis, Y.W. and Y.S.; Resources, Y.L. and Y.C.; Supervision, Z.Q.; Visualization, S.Q., P.W. and X.R.; Writing—original draft, Y.Z.; Writing—review and editing, Z.Q. All authors have read and agreed to the published version of the manuscript.

Funding: This research was funded by subsidy funds of Jiangsu Province for joint prevention and control of *Ulva prolifera* green tide in 2023; Research and application demonstration of Jiangsu coastal zone resource remote sensing monitoring method based on multi-source remote sensing data, grant number: JSZRHYKJ202207; Study on intelligent recognition and spatiotemporal variation of *Ulva prolifera* in Jiangsu sea area by satellite remote sensing, grant number: KJXM2019042.

Data Availability Statement: All data generated or analyzed during this study are included in this published article.

Acknowledgments: Thanks to the HY-1C/D satellite images provided by the National Satellite Ocean Application Service of China.

Conflicts of Interest: The authors declare no conflicts of interest.

References

- Ye, N.H.; Zhang, X.W.; Mao, Y.Z.; Liang, C.W.; Xu, D.; Zou, J.; Zhuang, Z.M.; Wang, Q.Y. 'Green tides' are overwhelming the coastline of our blue planet: Taking the world's largest example. *Ecol. Res.* **2011**, *26*, 477–485. [[CrossRef](#)]
- Liu, D.; Keesing, J.K.; Dong, Z.; Zhen, Y.; Di, B.; Shi, Y.; Fearn, P.; Shi, P. Recurrence of the world's largest green-tide in 2009 in Yellow Sea, China: *Porphyra yezoensis* aquaculture rafts confirmed as nursery for macroalgal blooms. *Mar. Pollut. Bull.* **2010**, *60*, 1423–1432. [[CrossRef](#)] [[PubMed](#)]
- Pang, S.J.; Liu, F.; Shan, T.F.; Xu, N.; Zhang, Z.H.; Gao, S.Q.; Chopin, T.; Sun, S. Tracking the algal origin of the *Ulva* bloom in the Yellow Sea by a combination of molecular, morphological and physiological analyses. *Mar. Environ. Res.* **2010**, *69*, 207–215. [[CrossRef](#)] [[PubMed](#)]
- Liu, F.; Pang, S.J.; Zhao, X.B.; Hu, C.M. Quantitative, molecular and growth analyses of *Ulva* microscopic propagules in the coastal sediment of Jiangsu province where green tides initially occurred. *Mar. Environ. Res.* **2012**, *74*, 56–63. [[CrossRef](#)] [[PubMed](#)]
- Hu, C.; Li, D.; Chen, C.; Ge, J.; Muller-Karger, F.E.; Liu, J.; Yu, F.; He, M.X. On the recurrent *Ulva prolifera* blooms in the Yellow Sea and East China Sea. *J. Geophys. Res. Ocean.* **2010**, *115*. [[CrossRef](#)]
- Zhang, J.; Huo, Y.; Wu, H.; Yu, K.; Kim, J.K.; Yarish, C.; Qin, Y.; Liu, C.; Xu, R.; He, P. The origin of the *Ulva* macroalgal blooms in the Yellow Sea in 2013. *Mar. Pollut. Bull.* **2014**, *89*, 276–283. [[CrossRef](#)] [[PubMed](#)]
- Zhao, J.; Jiang, P.; Liu, Z.; Wei, W.; Lin, H.; Li, F.; Wang, J.; Qin, S. The Yellow Sea green tides were dominated by one species, *Ulva* (*Enteromorpha*) *prolifera*, from 2007 to 2011. *Chin. Sci. Bull.* **2013**, *58*, 2298–2302. [[CrossRef](#)]
- Bao, M.; Guan, W.; Yang, Y.; Cao, Z.; Chen, Q. Drifting trajectories of green algae in the western Yellow Sea during the spring and summer of 2012. *Estuar. Coast. Shelf Sci.* **2015**, *163*, 9–16. [[CrossRef](#)]
- Cui, T.-W.; Zhang, J.; Sun, L.-E.; Jia, Y.-J.; Zhao, W.; Wang, Z.-L.; Meng, J.-M. Satellite monitoring of massive green macroalgae bloom (GMB): Imaging ability comparison of multi-source data and drifting velocity estimation. *Int. J. Remote Sens.* **2012**, *33*, 5513–5527. [[CrossRef](#)]
- Xu, Q.; Zhang, H.; Cheng, Y.; Zhang, S.; Zhang, W. Monitoring and tracking the green tide in the Yellow Sea with satellite imagery and trajectory model. *IEEE J. Sel. Top. Appl. Earth Obs. Remote Sens.* **2016**, *9*, 5172–5181. [[CrossRef](#)]
- Liu, X.; Wang, Z.; Fan, S.; Zhang, X.; Li, R.; Li, Y. The distribution of green algal micro-propagules and macroalgae at the early stage of green tide in the coastal area of South Jiangsu Province in 2014. *J. Ocean Univ. China* **2017**, *16*, 81–86. [[CrossRef](#)]
- Xing, Q.; An, D.; Zheng, X.; Wei, Z.; Wang, X.; Li, L.; Tian, L.; Chen, J. Monitoring seaweed aquaculture in the Yellow Sea with multiple sensors for managing the disaster of macroalgal blooms. *Remote Sens. Environ.* **2019**, *231*, 111279. [[CrossRef](#)]
- Liu, F.; Pang, S.J.; Xu, N.; Shan, T.F.; Sun, S.; Hu, X.; Yang, J.Q. *Ulva* diversity in the Yellow Sea during the large-scale green algal blooms in 2008–2009. *Phycol. Res.* **2010**, *58*, 270–279. [[CrossRef](#)]
- Li, Y.; Song, W.; Xiao, J.; Wang, Z.; Fu, M.; Zhu, M.; Li, R.; Zhang, X.; Wang, X. Tempo-spatial distribution and species diversity of green algae micro-propagules in the Yellow Sea during the large-scale green tide development. *Harmful Algae* **2014**, *39*, 40–47. [[CrossRef](#)]
- Duan, W.; Guo, L.; Sun, D.; Zhu, S.; Chen, X.; Zhu, W.; Xu, T.; Chen, C. Morphological and molecular characterization of free-floating and attached green macroalgae *Ulva* spp. in the Yellow Sea of China. *J. Appl. Phycol.* **2012**, *24*, 97–108. [[CrossRef](#)]
- Song, W.; Peng, K.; Xiao, J.; Li, Y.; Wang, Z.; Liu, X.; Fu, M.; Fan, S.; Zhu, M.; Li, R. Effects of temperature on the germination of green algae micro-propagules in coastal waters of the Subei Shoal, China. *Estuar. Coast. Shelf Sci.* **2015**, *163*, 63–68. [[CrossRef](#)]
- Qi, L.; Hu, C.; Xing, Q.; Shang, S. Long-term trend of *Ulva prolifera* blooms in the western Yellow Sea. *Harmful Algae* **2016**, *58*, 35–44. [[CrossRef](#)] [[PubMed](#)]
- Zhang, T.; Wang, X. Release and microbial degradation of dissolved organic matter (DOM) from the macroalgae *Ulva prolifera*. *Mar. Pollut. Bull.* **2017**, *125*, 192–198. [[CrossRef](#)] [[PubMed](#)]
- Song, X.K.; Shi, Y.J.; Liu, A.Y.; Xing, H.Y.; Jiang, H.C.; Wang, W.J.; Zhang, L.M. The impact of green tide on the phytoplankton community in Yellow Sea. *Appl. Mech. Mater.* **2013**, *260*, 1130–1137. [[CrossRef](#)]
- Pereira, R.; Yarish, C. The role of *Porphyra* in sustainable culture systems: Physiology and applications. In *Seaweeds and Their Role in Globally Changing Environments*; Springer: Berlin/Heidelberg, Germany, 2010; pp. 339–354.

21. Kim, J.K.; Yarish, C.; Hwang, E.K.; Park, M.; Kim, Y.; Kim, J.K.; Yarish, C.; Hwang, E.K.; Park, M.; Kim, Y. Seaweed aquaculture: Cultivation technologies, challenges and its ecosystem services. *Algae* **2017**, *32*, 1–13. [[CrossRef](#)]
22. Charlier, R.H.; Morand, P.; Finkl, C.W.; Thys, A.C. Dealing with green tides on Brittany and Florida Coasts. In *International Symposium on Environmental Science and Technology*; HAL Open Science: Lyon, France, 2007; pp. 1435–1441.
23. Cai, L.; Zhou, M.; Liu, J.; Tang, D.; Zuo, J. HY-1C observations of the impacts of islands on suspended sediment distribution in Zhoushan coastal waters, China. *Remote Sens.* **2020**, *12*, 1766. [[CrossRef](#)]
24. Liu, J.; Liu, J.; Ding, J.; Lu, Y. A refined imagery algorithm to extract green tide in the Yellow Sea from HY-1C satellite CZI measurements. *Haiyang Xuebao* **2022**, *44*, 1–11.
25. Tang, L.; Lu, Y.; Jiao, J.; Liu, J.; Hu, L.; Ding, J.; Xing, Q.; Wang, F.; Song, Q.; Chen, Y.; et al. High-precision monitoring of green tide biomass in the Yellow Sea of China through optical remote sensing. *Natl. Remote Sens. Bull.* **2023**, *27*, 2484–2498.
26. Xing, Q.; Hu, C. Mapping macroalgal blooms in the Yellow Sea and East China Sea using HJ-1 and Landsat data: Application of a virtual baseline reflectance height technique. *Remote Sens. Environ.* **2016**, *178*, 113–126. [[CrossRef](#)]
27. Hu, C. A novel ocean color index to detect floating algae in the global oceans. *Remote Sens. Environ.* **2009**, *113*, 2118–2129. [[CrossRef](#)]
28. Huang, S.; Tang, L.; Hupy, J.P.; Wang, Y.; Shao, G.F. A commentary review on the use of normalized difference vegetation index (NDVI) in the era of popular remote sensing. *J. For. Res.* **2021**, *32*, 1–6. [[CrossRef](#)]
29. Xu, F.; Gao, Z.; Shang, W.; Jiang, X.; Zheng, X.; Ning, J.; Song, D. Validation of MODIS-based monitoring for a green tide in the Yellow Sea with the aid of unmanned aerial vehicle. *J. Appl. Remote Sens.* **2017**, *11*, 012007. [[CrossRef](#)]
30. Liu, D.; Yu, J. Otsu method and K-means. In *Proceedings of the 2009 Ninth International Conference on Hybrid Intelligent Systems*, Shenyang, China, 12–14 August 2009; IEEE: Piscataway, NJ, USA, 2009; Volume 1, pp. 344–349.
31. Gu, X.F.; Chen, X.F.; Yin, Q.; Li, Z.Q.; Xu, H.; Shao, Y.; Li, Z.W. Stereoscopic remote sensing used in monitoring enteromorpha prolifera disaster in chinese yellow sea. *Spectrosc. Spectr. Anal.* **2011**, *31*, 1627–1632.
32. Kim, K.; Shin, J.; Ryu, J.H. Application of multi-satellite sensors to estimate the green-tide area. *Korean J. Remote Sens.* **2018**, *34*, 339–349.
33. Yang, D.; Yuen, K.-V.; Gu, X.; Sun, C.; Gao, L. Influences of environmental factors on the dissipation of green tides in the Yellow Sea, China. *Mar. Pollut. Bull.* **2023**, *189*, 114737. [[CrossRef](#)] [[PubMed](#)]
34. Hu, L.; Hu, C.; He, M.-X. Remote estimation of biomass of *Ulva prolifera* macroalgae in the Yellow Sea. *Remote Sens. Environ.* **2017**, *192*, 217–227. [[CrossRef](#)]
35. Liu, D.; Keesing, J.K.; He, P.; Wang, Z.; Shi, Y.; Wang, Y. The world’s largest macroalgal bloom in the Yellow Sea, China: Formation and implications. *Estuar. Coast. Shelf Sci.* **2013**, *129*, 2–10. [[CrossRef](#)]
36. Xiao, Y.; Zhang, J.; Cui, T.; Gong, J.; Liu, R.; Chen, X.; Liang, X. Remote sensing estimation of the biomass of floating *Ulva prolifera* and analysis of the main factors driving the interannual variability of the biomass in the Yellow Sea. *Mar. Pollut. Bull.* **2019**, *140*, 330–340. [[CrossRef](#)] [[PubMed](#)]
37. Taylor, R.; Fletcher, R.L.; Raven, J.A. Preliminary studies on the growth of selected ‘green tide’algae in laboratory culture: Effects of irradiance, temperature, salinity and nutrients on growth rate. *Bot. Mar.* **2001**, *44*, 327–336. [[CrossRef](#)]
38. Lee, J.H.; Pang, I.C.; Moon, I.J.; Ryu, J.H. On physical factors that controlled the massive green tide occurrence along the southern coast of the Shandong Peninsula in 2008: A numerical study using a particle-tracking experiment. *J. Geophys. Res. Ocean.* **2011**, *116*. [[CrossRef](#)]
39. Xu, Q.; Zhang, H.; Ju, L.; Chen, M. Interannual variability of *Ulva prolifera* blooms in the Yellow Sea. *Int. J. Remote Sens.* **2014**, *35*, 4099–4113. [[CrossRef](#)]
40. Fan, S.; Fu, M.; Wang, Z.; Zhang, X.; Song, W.; Li, Y.; Liu, G.; Shi, X.; Wang, X.; Zhu, M. Temporal variation of green macroalgal assemblage on *Porphyra* aquaculture rafts in the Subei Shoal, China. *Estuar. Coast. Shelf Sci.* **2015**, *163*, 23–28. [[CrossRef](#)]
41. Teichberg, M.; Fox, S.E.; Olsen, Y.S.; Valiela, I.; Martinetto, P.; Iribarne, O.; Muto, E.Y.; Petti, M.A.V.; Corbisier, T.N.; Soto-Jimenez, M.F.; et al. Eutrophication and macroalgal blooms in temperate and tropical coastal waters: Nutrient enrichment experiments with *Ulva* spp. *Glob. Change Biol.* **2010**, *16*, 2624–2637. [[CrossRef](#)]
42. Nelson, T.A.; Haberlin, K.; Nelson, A.V.; Ribarich, H.; Hotchkiss, R.; Van Alstyne, K.L.; Buckingham, L.; Simunds, D.J.; Fredrickson, K. Ecological and physiological controls of species composition in green macroalgal blooms. *Ecology* **2008**, *89*, 1287–1298. [[CrossRef](#)] [[PubMed](#)]

Disclaimer/Publisher’s Note: The statements, opinions and data contained in all publications are solely those of the individual author(s) and contributor(s) and not of MDPI and/or the editor(s). MDPI and/or the editor(s) disclaim responsibility for any injury to people or property resulting from any ideas, methods, instructions or products referred to in the content.